Improved Maneuverability for Multirotor Aerial Vehicles using Globally Stabilizing Feedbacks

Pedro Casau, Rita Cunha and Carlos Silvestre

?***Abstract*—In this paper, we present the design of trajectory tracking controllers for multirotor aerial vehicles that have the ability to operate both with and without thrust reversal. We follow a hierarchical control approach, in the sense that we start by designing a common saturated controller for the position subsystem and use it to provide a reference to an attitude tracking controller. The controllers for each operating mode are able to achieve global asymptotic stability as well as semiglobal exponential stabilization of the zero tracking error set. We demonstrate the capabilities of the proposed controllers in a simulation that performs a throw-and-catch maneuver.**

I. Introduction

Nowadays, Uninhabited Aerial Vehicles (UAVs) can be bought in consumer electronic stores and piloted by the whisk of a smartphone. High power density batteries opened the skies to these remotely operated aerial vehicles and the development of new sensors, processors and actuators is fueling further innovation. A few of the areas of soaring research include: parcel delivery, video capture, entertainment, surveillance, infrastructure inspection and transportation (c.f. [1], [2], [3] and [4]). The class of UAVs known as *multirotor aerial vehicles* is one of the most popular solutions to these applications. These vehicles are equipped with several propellers that produce thrust and torque (see Figure 1). The simplicity of their mechanical design is in deep contrast with the control challenges that it poses. These difficulties lead to a decade long research effort described in [5] and [6] and that we summarize below.

The contributions in [7], [8] and [9] focus on the development and validation of dynamical models for multirotor aerial vehicles. In these papers, the controller has a PID structure with gains that are tuned for a limited region of the flight envelope. In this paper, we follow a control design approach that is more closely related to [10] and the line of research that originated from it. The main features of said line of research consist of a combination of hierarchical control with geometric feedback as described below:

P. Casau and R. Cunha are with the Department of Electrical and Computer Engineering at Instituto Superior Técnico, Universidade de Lisboa, Lisboa, Portugal. E-mail addresses: {pcasau,rcunha}@isr.tecnico.ulisboa.pt C. Silvestre is with the Department of Electrical and Computer Engineering of the Faculty of Science and Technology of the University of Macau, Macau, China, and with Instituto Superior Técnico, Universidade de Lisboa, Lisboa, Portugal. E-mail address: csilvestre@um.edu.mo This work was partially supported by the projects MYRG2018-00198-FST and MYRG2016-00097-FST of the University of Macau; by the Macau Science and Technology, Development Fund under Grant FDCT/026/2017/A1 and by Fundação para a Ciência e a Tecnologia (FCT) through Project UID/EEA/50009/2019, and LOTUS PTDC/EEI-AUT/5048/2014 and grant CEECIND/04652/2017.

1) Hierarchical Control Architecture: given a desired (smooth) position trajectory, the hierarchical control architecture consists of designing a *virtual* feedback law at the acceleration level and using it to define an attitude reference that is to be tracked by an inner attitude tracking controller.

2) Geometric Feedback: we say that the feedback law is *geometric* if it takes into account the topology of the space of the attitude representation unlike linearization approaches, which discard that information.

Some important contributions to multirotor control that share the aforementioned characteristics are given in [11], [12], [13] and [14]. The proposed approach differs from solutions that focus solely on attitude stabilization, such as the ones in [15] and [16]. For an in-depth comparison between mutirotor control strategies, we refer the reader to [17].

Off-the-shelf multirotor vehicles usually have a number of different modes of operation. For example, the *Blade 200qx* quadrotor vehicle has the following operating modes: 1) position stabilization mode; 2) angle stabilization mode; 3) aerobatic mode. Depending on the operating mode, the internal controller maps Radio Frequency (RF) commands to position, angle or angular velocity commands. It is seldom the case that off-the-shelf multirotor vehicles allow for direct torque control, much less individual rotor control.

In this paper, we develop higher level controls for off-the-shelf multirotor vehicles that have similar functions to the *Blade 200qx* quadrotor of Figure 1. Namely, we assume that the input to the system is comprised of the thrust and angular velocity commands and we assume that the vehicle is capable of operating with or without thrust reversal. Using the concept of synergistic potential functions that was introduced in [18] we expand the contributions in [19] and [20] in the following ways: 1) we provide a smooth saturated feedback law for the position subsystem whose parameters can be selected to simultaneously achieve global asymptotic stabilization and semiglobal exponential stabilization of the zero tracking error set; 2) we demonstrate these stability properties can be extended to the full dynamical system by

Fig. 1. Blade 200qx quadrotor in inverted flight.

means of synergistic hybrid feedback. In particular, we use different synergistic potential functions when thrust reversal is available and when it is not, which lead to very different behavior of the closed loop system. The behavior of the closed-loop systems is illustrated with simulations of throw-and-catch maneuvers.

This paper is organized as follows: Section II presents the notation and mathematical concepts that are used throughout the paper; Section III formally introduces the problem at hand; Section IV presents the design of the controller for the position subsystem; Section V completes the controller design for the full system using synergistic hybrid feedback with and without thrust reversal; Section VII presents the conclusions of the paper. The proofs of the results in this paper were omitted due to space constraints, but will appear elsewhere.

II. Preliminaries and Notation

$\mathbb{N}$ denotes the natural numbers and 0. Given $n, m \in \mathbb{N}$: $\mathbb{R}^n$ denotes the n-dimensional Euclidean space with norm $|x| := \sqrt{x^\top x}$ for each $x \in \mathbb{R}^n$; $\mathbf{1}_n \in \mathbb{R}^n$ denotes an n-dimensional vector of ones; $0_n \in \mathbb{R}^n$ denotes the n-dimensional zero vector; $\mathbf{e}_i \in \mathbb{R}^n$ is defined for each $i \in \{1, 2, \ldots, n\}$ and represents a vector whose entries are all zero except for the i-th component which is equal to 1; $\mathbb{R}^{m\times n}$ denotes the space of $m \times n$ matrices; I_n denotes the $n \times n$ identity matrix $0_{m\times n}$ denotes an $m \times n$ matrix of zeros; the special orthogonal group is $\mathsf{SO}(\mathsf{n}) := \{R \in \mathbb{R}^{n\times n} : R^\top R = I_n, \det(R) = 1\}$; the n-dimensional sphere is represented by $\mathsf{S}^n := \{x \in \mathbb{R}^{n+1} : x^\top x = 1\}$; a set-valued mapping M from $\mathbb{R}^m$ to $\mathbb{R}^n$ is denoted by $M : \mathbb{R}^m \rightrightarrows \mathbb{R}^n$ and it is a function that maps vectors in $x \in \mathbb{R}^m$ to subsets of $\mathbb{R}^n$, i.e., $M(x) \subset \mathbb{R}^n$ for each $x \in \mathbb{R}^m$; the closed n-dimensional ball centered at c with radius γ is denoted by $c + \gamma bB := \{x \in \mathbb{R}n : |x - c| \leq \gamma\}$. Given a set $S \subset \mathbb{R}^n$, we define $S + \gamma bB := \bigcup_{s\in S}(s + \gamma bB)$. Given $v = (v_1, v_2, \ldots, v_n) \in \mathbb{R}^n$, the mapping $v \to \operatorname{diag}(v)$ represents the diagonal matrix whose diagonal entries are the components of v. If $v_i < 0$ for each $i \in \{1, 2, \ldots, n\}$, then we write $v \prec 0_n$. Given a set-valued mapping $M : \mathbb{R}^m \rightrightarrows \mathbb{R}^n$, we define $\operatorname{rge} M := \{y \in \mathbb{R}^n : \exists x \in \mathbb{R}^m \text{ such that } y \in M(x)\}$.

Let $P \in \mathbb{R}^{n\times n}$. if $P = P^\top$, then P is said to be symmetric. Real symmetric matrices have real eigenvalues and we denote the highest and lowest eigenvalue of P by $\lambda_{max}(P)$ and $\lambda_{min}(P)$, respectively. A symmetric matrix $P \in \mathbb{R}^{n\times n}$ is said to be *positive definite* if all of its eigenvalues are positive, in which case we write $P \succ 0_{n\times n}$. A symmetric matrix P is said to be *positive semidefinite* if all of its eigenvalues are nonnegative, in which case we write $P \succeq 0_{n\times n}$. Given $A \in \mathbb{R}^{m\times n}$, $\operatorname{vec}(A) = \begin{bmatrix}\mathbf{e}_1{}^\top A^\top & \mathbf{e}_2{}^\top A^\top & \ldots & \mathbf{e}_n{}^\top A\end{bmatrix}^\top$. Given a continuously differentiable function $F : \mathbb{R}^{m\times n} \to \mathbb{R}^{p\times q}$, $\mathcal{D}F(X) := \dfrac{\partial \operatorname{vec}(F)}{\partial \operatorname{vec}(X)^\top}(X)$ for each $X \in \mathbb{R}^{m\times n}$ A function $V : \mathbb{R}^n \to \mathbb{R}_{\geq 0}$ is said to be positive definite relative to $\mathcal{A}$ if $V(x) = 0 \iff x \in \mathcal{A}$, where $\mathbb{R}_{\geq 0}$ represents the nonnegative real numbers. If $\mathcal{A} = \{0\}$, then we say that V is positive definite and if, for each sequence $\{x_i\}_{i\in\mathbb{N}}$ satisfying $|x_i|_{\mathcal{A}} \to +\infty$, we have $V(x_i) \to +\infty$ then we say that V is radially unbounded, where $|x|_{\mathcal{A}} = \inf\{|x - y| : y \in \mathcal{A}\}$ represent the minimum distance between $x \in \mathbb{R}^n$ and $\mathcal{A}$.

Definition 1. *Given compact sets $\mathcal{Q}$ and $\mathcal{A} \subset \mathsf{S}^n \times \mathcal{Q}$, a continuously differentiable function $V : \mathsf{S}^n \times \mathcal{Q} \to \mathbb{R}_{\geq 0}$ is said to be a* synergistic potential function *on S^n relative to $\mathcal{A}$ if it is positive definite relative to $\mathcal{A}$ and there exists $\delta > 0$ such that*

$$\mu_V(x, q) := V(x, q) - \min\{V(x, q) : q \in \mathcal{Q}\} > \delta \tag{1}$$

for each $(x, q) \in \mathcal{E}_V \backslash \mathcal{A}$, with $\mathcal{E}_V := \{(x, q) \in \mathsf{S}^n \times \mathcal{Q} : \Pi(x)\nabla V(x, q) = 0_{n+1}\}$ and $\Pi(x) := I_{n+1} - xx^\top$ for each $x \in \mathsf{S}^n$ and $\nabla V(x, q) := \frac{\partial V}{\partial x}(x, q)$ for each $(x, q) \in \mathsf{S}^n \times \mathcal{Q}$. In addition, if (1) *is verified, we also say that V has* synergy gap exceeding δ.

Given a synergistic potential function on S^n relative to $\mathcal{A} \subset \mathsf{S}^n \times \mathcal{Q}$ with synergy gap exceeding δ, we define:

$$C_V := \{(x, q) \in \mathsf{S}^n \times \mathcal{Q} : \mu_V(x, q) \leq \delta\}, \tag{2a}$$
$$D_V := \{(x, q) \in \mathsf{S}^n \times \mathcal{Q} : \mu_V(x, q) \geq \delta\}. \tag{2b}$$

III. Problem Setup

The dynamics of a thrust vectored vehicle can be described by

$$\dot{p} = v \tag{3a}$$
$$m\dot{v} = RrT + mg \tag{3b}$$
$$\dot{R} = RS(\omega) \tag{3c}$$

where $S(\omega)$ is such that $S(\omega)v = \omega \times v$ for all $\omega, v \in \mathbb{R}^3$, $p \in \mathbb{R}^3$ and $v \in \mathbb{R}^3$ denote the position and the velocity of the vehicle with respect to the inertial reference frame (in inertial coordinates), $R \in \mathsf{SO}(3)$ is the rotation matrix that maps vectors in body-fixed coordinates to inertial coordinates, $g \in \mathbb{R}^3$ represents the gravity vector and $r \in \mathsf{S}^2$ is the thrust vector in body-fixed coordinates. Furthermore, the inputs to (3) are $\omega \in \mathbb{R}^3$ and $T \in \mathbb{R}$ which represent the angular velocity in body-fixed coordinates and the magnitude of the thrust, respectively. The dynamical model (3) is a simplification of the one provided in [10] that better suits our experimental setup. Suppose that we are given a reference trajectory satisfying the following assumption.

Assumption 1. *The reference trajectory $t \mapsto p_d(t)$ is a thrice continuously differentiable path defined for each $t \geq 0$ that satisfies $\operatorname{rge} p_d^{(3)} \subset \mathcal{R}_3$ for some compact and convex set $\mathcal{R}_3 \subset \mathbb{R}^3$ and $\operatorname{rge} \ddot{p_d} \subset \mathcal{R}_2$ for some compact set $\mathcal{R}_2 \subset \mathbb{R}^3$.*

Given a reference trajectory that satisfies Assumption 1, we define the tracking errors

$$e_p := p - p_d \tag{4a}$$
$$e_v := v - \dot{p_d} \tag{4b}$$

whose dynamics can be derived from (3) and are given by:

$$\dot{e_p} = e_v, \quad \dot{e_v} = \frac{RrT}{m} + g - \ddot{p_d}. \tag{5}$$

If we assume that we have full control over $R \in \mathsf{SO}(3)$ and $T \in \mathbb{R}$, then it is possible to reduce the trajectory tracking problem to the problem of stabilizing a double integrator. This is the approach that we follow in the next section.

IV. Controller for the Position Subsystem

Let $\ell := (\ell_1, \ell_2, \ell_3) \in \mathbb{R}^3$ denote a vector with positive components and let $\sigma(u) := \begin{bmatrix}\sigma_1(u_1) & \sigma_2(u_2) & \sigma_3(u_3)\end{bmatrix}^\top$ represent a function that is defined for each $u := (u_1, u_2, u_3) \in \mathbb{R}^3$, with σ_i continuously differentiable, strictly increasing and satisfying

$$\sigma_i(u_i) = u_i \qquad \forall u_i \in [-\ell_i, \ell_i] \tag{6}$$

for each $i \in \{1, 2, 3\}$.

Example 1. *Given $\ell := (\ell_1, \ell_2, \ell_3) \in \mathbb{R}^3$ and $M := (M_1, M_2, M_3) \in \mathbb{R}^3$ satisfying $\ell_i < M_i$ $\forall i \in \{1, 2, 3\}$, the function*

$$\sigma_i(u_i) := \begin{cases} -\ell_i + \frac{2(M_i - \ell_i)}{\pi} \arctan\left(\frac{\pi(u_i + \ell_i)}{2(M_i - \ell_i)}\right) & \text{if } u_i < -\ell_i \\ u_i & \text{if } |u_i| \leq \ell_i \\ \ell_i + \frac{2(M_i - \ell_i)}{\pi} \arctan\left(\frac{\pi(u_i - \ell_i)}{2(M_i - \ell_i)}\right) & \text{if } u_i > \ell_i \end{cases}$$

is defined for each $u_i \in \mathbb{R}$ and it is strictly increasing, continuously differentiable and satisfies (6).

The function σ can be used to generate a reference for the thrust vector as follows

$$r_d(\ddot{p_d}, e) := \frac{\eta(\ddot{p_d}, e)}{|\eta(\ddot{p_d}, e)|} \tag{7}$$

with $e := (e_p, e_v) \in \mathbb{R}^6$,

$$\eta(\ddot{p_d}, e) = \sigma(Ke) + g - \ddot{p_d} \tag{8}$$

for each $(\ddot{p_d}, e) \in \mathcal{R}_2 \times \mathbb{R}^6$ such that $\eta(\ddot{p_d}, e) \neq 0$ and $K \in \mathbb{R}^{3\times 6}$. The following assumption guarantees that r_d in (7) is always well-defined.

Assumption 2. *Given $g \in \mathbb{R}^3$ as in* (3) *and a reference trajectory satisfying Assumption 1, the following holds*

$$\sigma(u) + g - \ddot{p_d} \neq 0_3 \qquad \forall (u, \ddot{p_d}) \in \mathbb{R}^3 \times \mathcal{R}_2.$$

If $RrT/m \equiv \eta(\ddot{p_d}, e)$, then (5) can be written as

$$\dot{e} = Ae + B\sigma(Ke), \tag{9}$$

with

$$A := \begin{bmatrix} 0_{3\times 3} & I_3 \\ 0_{3\times 3} & 0_{3\times 3} \end{bmatrix} \quad B := \begin{bmatrix} 0_{3\times 3} \\ I_3 \end{bmatrix}.$$

Using $e_p = (e_{p,1}, e_{p,2}, e_{p,3})$, $e_v = (e_{v,1}, e_{v,2}, e_{v,3})$ and

$$K = \begin{bmatrix} k_{1,1} & 0 & 0 & k_{1,2} & 0 & 0 \\ 0 & k_{2,1} & 0 & 0 & k_{2,2} & 0 \\ 0 & 0 & k_{3,1} & 0 & 0 & k_{3,2} \end{bmatrix}, \tag{10}$$

with $k_i := (k_{i,1}, k_{i,2}) \prec 0_2$ for each $i \in \{1, 2, 3\}$, the system (9) becomes a collection of three parallel double integrators, each of which is characterized by the dynamics $\dot{e_i} = (e_{v,i}, \sigma_i(k_i^\top e_i))$ where $e_i := (e_{p,i}, e_{v,i}) \in \mathbb{R}^2$ for each $i \in \{1, 2, 3\}$. In the next lemma, we present a Lyapunov function candidate for each double integrator that has a number of properties that are used in the sequel.

Lemma 1. *For each $i \in \{1, 2, 3\}$, $\ell_{p,i} > 0$, $\ell_i > 0$ and $k_i \prec 0_2$, there exists $P_i \succ 0_{2\times 2}$ such that:*

(P1) The function $V_{p,i}$, defined for each $e_i \in \mathbb{R}^2$, as follows:

$$V_{p,i}(e_i) := \frac{\epsilon_i}{2} \begin{bmatrix} \sigma_i(k_i^\top e_i) \\ e_{v,i} \end{bmatrix}^\top P_i \begin{bmatrix} \sigma_i(k_i^\top e_i) \\ e_{v,i} \end{bmatrix} + \epsilon_i \int_0^{k_i^\top e_i} \sigma(\tau) d\tau$$

with

$$\epsilon_i = \frac{2\ell_{p,i}}{\ell_i^2}$$

is continuously differentiable, positive definite and radially unbounded;

(P2) There exists a positive definite function $W_{p,i} : \mathbb{R}^2 \to \mathbb{R}_{\geq 0}$ such that

$$\mathcal{D}V_{p,i}(e_i) \begin{bmatrix} e_{v,i} \\ \sigma_i(k_i^\top e_i) \end{bmatrix} \leq -W_{p,i}(e_i)$$

for each $e_i \in \mathbb{R}^2$;

(P3) Each e_i in

$$\Omega_{V_{p,i}}(\ell_{p,i}) := \{e_i \in \mathbb{R}^2 : V_{p,i}(e_i) \leq \ell_{p,i}\} \tag{11}$$

satisfies $\left|k_i^\top e_i\right| \leq \ell_i$;

(P4) There exists $\lambda_{p,i} > 0$ such that $\mathcal{D}V_{p,i}(e_i) \begin{bmatrix} e_{v,i} \\ \sigma_i(k_i^\top e_i) \end{bmatrix} \leq -\lambda_{p,i} V_{p,i}(e_i)$ for all $e_i \in \mathbb{R}^2$ satisfying $k_i^\top e_i \leq \ell_i$;

(P5) There exist $\overline{\alpha}_i \geq \underline{\alpha}_i > 0$ such that $\underline{\alpha}_i |e_i|^2 \leq V_{p,i}(e_i) \leq \overline{\alpha}_i |e_i|^2$ for all $e_i \in \mathbb{R}^2$ satisfying $k_i^\top e_i \leq \ell_i$;

(P6) There exists a continuous function $\rho_i : \mathbb{R}^2 \to \mathbb{R}_{\geq 0}$ such that

$$\left|\frac{\partial V_{p,i}(e_i)}{\partial e_{v,i}}\right| (V_{p,i}(e_i))^{-\frac{1}{2}} \leq \rho_i(e_i)$$

for each $e_i \in \mathbb{R}^2$.

Properties (P1) and (P2) can be used to prove that the origin of (9) is globally asymptotically stable. Together with property (P3), we have that solutions to (9) starting in the sublevel set (11) do not exceed the bounds ℓ_i in (6). Properties (P4) and (P5) allow for semiglobal exponential stability, as shown in the following sections.

V. Global Asymptotic Tracking

A. With Thrust Reversal

We start the controller design with the construction of a synergistic potential function on S^2.

Lemma 2. *Let $\delta_1 \in (0, 2)$, $\mathcal{Q}_1 := \{-1, 1\}$ and $\mathcal{A}_1 := \{(x, q_1) \in \mathsf{S}^2 \times \mathcal{Q}_1 : x = q_1 r\}$ with $r \in \mathsf{S}^2$ given in* (3)*. The function $V_1(x, q_1) := 1 - q_1 x^\top r$ is a synergistic potential function on S^2 relative to $\mathcal{A}_1$ with synergy gap exceeding δ_1. Moreover, there exists $\lambda_1 > 0$ such that*

$$|\Pi(x)\nabla V_1(x, q_1)|^2 \geq \lambda_1 V_1(x, q_1)$$

for each $x \in C_{V_1}$.

Let $z_1 := (\ddot{p_d}, e, R, q_1) \in \mathcal{Z}_1 := \mathcal{R}_2 \times \mathbb{R}^6 \times \mathsf{SO(3)} \times \mathcal{Q}_1$. We define the hybrid controller

$$\dot{q}_1 = 0 \qquad z \in C_1 := \{z_1 \in \mathcal{Z}_1 : (R^\top r_d(\ddot{p_d}, e), q_1) \in C_{V_1}\}$$

$$q_1^+ = -q_1 \quad z \in D_1 := \{z_1 \in \mathcal{Z}_1 : (R^\top r_d(\ddot{p_d}, e), q_1) \in D_{V_1}\},$$

where μ_{V_1} is given in (1) and C_{V_1}, D_{V_1} are given in (2).

Given σ as in Section III, $K \in \mathbb{R}^{3\times 6}$ as in (10) and

$$V_p(e) := \sum_{i=1}^{3} V_{p,i}(e_i)$$

for each $e \in \mathbb{R}^6$, we assign the input T of (3) to

$$T_1(\ddot{p_d}, e, R) = m\, r^\top R^\top \eta(\ddot{p_d}, e) \qquad \forall (\ddot{p_d}, e, R) \in \mathcal{R}_2 \times \mathbb{R}^6 \times \mathsf{SO(3)} \tag{13}$$

with $\eta(\ddot{p_d}, e)$ given in (8), hence T can take both positive as well as negative values. Moreover, we assign the input ω of (3) to

$$\omega_1(p_d^{(3)}, z_1) = -S(r)^2 \Big(q_1 \beta_1 S(r) R^\top r_d(\ddot{p_d}, e) - \frac{q_1 \nu(\ddot{p_d}, e, R)}{\alpha} + S(R^\top r_d(\ddot{p_d}, e)) \frac{R^\top \dot{\eta}_1(p_d^{(3)}, \ddot{p_d}, e)}{|\eta(\ddot{p_d}, e)|} \Big) \qquad \forall (p_d^{(3)}, z_1) \in \mathcal{R}_3 \times \mathcal{Z}_1$$

with $\alpha, \beta_1 > 0$,

$$\dot{\eta}_1(p_d^{(3)}, \ddot{p_d}, e) \equiv \mathcal{D}\eta(\ddot{p_d}, e) \begin{bmatrix} p_d^{(3)} \\ e_v \\ \frac{RrT_1(\ddot{p_d}, e, R)}{m} + g - \ddot{p_d} \end{bmatrix}$$

and $\nu(\ddot{p_d}, e, R) := |\eta(\ddot{p_d}, e)|\, S(r) R^\top B^\top \mathcal{D} V_p(e)^\top$ for each $(\ddot{p_d}, e, R) \in \mathcal{R}_2 \times \mathbb{R}^6 \times \mathsf{SO(3)}$. The closed-loop system is given by the hybrid system $\mathcal{H}_1 := (C_1, F_1, D_1, G_1)$[1] with

$$F_1(z_1) := \left\{ \begin{pmatrix} p_d^{(3)} \\ e_v \\ \frac{RrT_1(\ddot{p_d}, e, R)}{m} + g - \ddot{p_d} \\ RS(\omega_1(p_d^{(3)}, z_1)) \\ 0 \end{pmatrix} : p_d^{(3)} \in \mathcal{R}_3 \right\}$$

for each $z_1 \in C_1$ and $G_1(z_1) := (\ddot{p_d}, e, R, -q)$ for each $z_1 \in D_1$. The next result asserts the global asymptotic stability of the zero tracking error set for the closed-loop system $\mathcal{H}_1$. We refer the reader to a similar proof in [22].

Proposition 1. *Let Assumptions 1 and 2 hold and let K be given by* (10)*. The set*

$$\mathcal{B}_1 := \{ z_1 \in \mathcal{Z}_1 : e = 0,\ (R^\top r_d(\ddot{p_d}, e), q_1) \in \mathcal{A}_1 \}$$

is globally asymptotically stable for $\mathcal{H}_1$.

In addition to global asymptotic stability of $\mathcal{B}_1$ for $\mathcal{H}_1$, we also show that $\mathcal{B}_1$ is: 1) *locally exponentially stable for* $\mathcal{H}_1$, because there exists a neighborhood of $\mathcal{B}_1$ from which solutions converge exponentially to $\mathcal{B}_1$; 2) *semiglobally exponentially stable for* $\mathcal{H}_1$, because, for each compact set of initial conditions $(e, R)(0,0) \in \Omega \subset \mathbb{R}^6 \times \mathsf{SO(3)}$, there exists a controller gain K that guarantees exponential convergence to $\mathcal{B}_1$ for solutions starting in that set.

Proposition 2. *Let Assumptions 1 and 2 hold and let K be given by* (10)*. There exist $c, \lambda, \gamma > 0$ such that, for each solution ϕ to $\mathcal{H}_1$ with initial condition $\phi(0,0) \in (\mathcal{B}_1 + \gamma b B) \cap \mathcal{Z}_1$, the following holds*

$$|\phi(t,j)|_{\mathcal{B}_1} \le c\, |\phi(0,0)|_{\mathcal{B}_1} \exp(-\lambda t) \tag{14}$$

for all $(t,j) \in \operatorname{dom}\phi$.

Proposition 3. *Let Assumptions 1 and 2 hold and let K be given by* (10)*. For each compact set $\Omega \subset \mathbb{R}^6 \times \mathsf{SO(3)}$ there exist $c, \lambda > 0$ and $k_i \in \mathbb{R}^2$ for all $i \in \{1,2,3\}$ such that, for each solution ϕ to $\mathcal{H}_1$ with initial condition $\phi(0,0) \in \mathcal{R}_2 \times \Omega \times \mathcal{Q}_1$,* (14) *holds for all $(t,j) \in \operatorname{dom}\phi$.*

Semiglobal exponential stability is achieved in Proposition 3 through a low gain design, meaning that it is possible to encompass larger and larger compact sets of initial conditions choosing smaller and smaller control gains K, but this has adverse effects on the convergence rate of the position subsystem. In the next section, we design a controller for the case without thrust reversal.

B. Without Thrust Reversal

We start with the assumption that there exists a synergistic potential function relative to r.

Assumption 3. *Given a compact set $\mathcal{Q}_2$ and $\mathcal{A}_2 := \{r\} \times \mathcal{Q}_2$ with $r \in \mathsf{S}^2$ as in* (3)*, there exists a synergistic potential function $V_2 : \mathsf{S}^2 \times \mathcal{Q}_2 \to \mathbb{R}_{\ge 0}$ relative to $\mathcal{A}_2$ with synergy gap exceeding δ satisfying*

$$c_1 |(x, q_2)|_{\mathcal{A}_2}^2 \le V_2(x,q) \le c_2 |(x,q_2)|_{\mathcal{A}_2}^2 \quad \forall (x, q_2) \in \mathsf{S}^2 \tag{15a}$$

$$|\Pi(x) \nabla V_2(x, q_2)|^2 \ge c_3 V_2(x, q_2) \qquad \forall (x, q_2) \in C_{V_2} \tag{15b}$$

for some $c_1, c_2, c_3 > 0$, where C_{V_2} is given in (2a)*.*

Example 2. *It is shown in [18] that the function*

$$V_2(x, q_2) := \frac{1 - r^\top x}{2 - r^\top x - q_2^\top x} \qquad \forall (x, q_2) \in \mathsf{S}^2 \times \mathcal{Q}_2$$

with $\mathcal{Q}_2 := \{ q_2 \in \mathsf{S}^2 : q_2^\top r \le 0 \}$ satisfies Assumption 3.

Under Assumption 3, let $z_2 := (\ddot{p_d}, e, R, q_2) \in \mathcal{Z}_2 := \mathcal{R}_2 \times \mathbb{R}^6 \times \mathsf{SO(3)} \times \mathcal{Q}_2$ and the hybrid controller

$$\begin{aligned} \dot{q}_2 &= 0 && z_2 \in C_2 \\ q_2^+ &\in \varrho(R^\top r_d(\ddot{p_d}, e)) && z_2 \in D_2, \end{aligned}$$

with

$$z_2 \in C_2 := \{ z_2 \in \mathcal{Z}_2 : (R^\top r_d(\ddot{p_d}, e), q_2) \in C_{V_2} \}$$
$$z_2 \in D_2 := \{ z_2 \in \mathcal{Z}_2 : (R^\top r_d(\ddot{p_d}, e), q_2) \in D_{V_2} \}$$

and $\varrho(x) := \arg\min \{ V_2(x,q) : q \in \mathcal{Q}_2 \}$ for each $x \in \mathsf{S}^2$.

Let $\alpha > 0$ and ν_2 denote a continuous function satisfying

$$\alpha \sqrt{c_1} c_3 \nu_2(\ddot{p_d}, e) \ge |\eta(\ddot{p_d}, e)|\, \rho(e)$$

for each $(\ddot{p_d}, e) \in \mathcal{R}_2 \times \mathbb{R}^6$ with

$$\rho(e) := \sum_{i=1}^{3} \rho_i(e_i) \quad \forall e \in \mathbb{R}^6$$

and ρ_i given in Lemma 1. Given η in (8), we assign the input T in (3) to

$$T_2(\ddot{p_d}, e) = m\, |\eta(\ddot{p_d}, e)| \quad \forall (\ddot{p_d}, e) \in \mathcal{R}_2 \times \mathbb{R}^6$$

[1]For more details on the framework of hybrid dynamical systems, we refer the reader to [21].

and the input ω in (3) to

$$\omega_2(p_d^{(3)}, z) = S(R^\top r_d(\ddot{p_d}, e))\Big(\frac{R^\top \dot{\eta}_2(p_d^{(3)}, z_2)}{|\eta(\ddot{p_d}|} + (\beta_2 + \nu_2(\ddot{p_d}, e))\nabla V_2(R^\top r_d(\ddot{p_d}, e), q_2)\Big)$$

for each $(p_d^{(3)}, z_2) \in \mathcal{R}_3 \times \mathcal{Z}_2$, with $\beta_2 > 0$ and

$$\dot{\eta}_2(p_d^{(3)}, z_2) \equiv \mathcal{D}\eta(\ddot{p_d}, e) \begin{bmatrix} p_d^{(3)} \\ e_v \\ \frac{RrT_2(\ddot{p_d}, e, R)}{m} + g - \ddot{p_d} \end{bmatrix}.$$

The closed-loop system is given by the hybrid system $\mathcal{H}_2 := (C_2, F_2, D_2, G_2)$ with data

$$F_2(z_2) := \left\{ \begin{bmatrix} p_d^{(3)} \\ e_v \\ \frac{RrT_2(\ddot{p_d}, e, R)}{m} + g - \ddot{p_d} \\ RS(\omega_2(p_d^{(3)}, z_2)) \\ 0 \end{bmatrix} : p_d^{(3)} \in \mathcal{R}_3 \right\}$$

for each $z_2 \in C_2$ and $G_2(z_2) := (\ddot{p_d}, e, R, \varrho(R^\top r_d(\ddot{p_d}, e))$ for each $z_2 \in D_2$. The following proposition shows that the zero tracking error set is globally asymptotically stable for the closed-loop system $\mathcal{H}_2$.

Proposition 4. *Let Assumptions 1 and 2 hold and let K be given by* (10)*. For each $k_i \prec 0_2$ and each $i \in \{1, 2, 3\}$, the set*

$$\mathcal{B}_2 := \{z_2 \in \mathcal{Z}_2 : e = 0,\ (R^\top r_d(\ddot{p_d}, e), q_2) \in \mathcal{A}_2\}$$

is globally asymptotically stable for $\mathcal{H}_2$.

Proposition 5. *Let Assumptions 1 and 2 hold and let K be given by* (10)*. For each $k_i \prec 0_2$ and each $i \in \{1, 2, 3\}$, there exist $c, \lambda, \gamma > 0$ such that, for each solution ϕ to $\mathcal{H}_2$ with initial condition $\phi(0, 0) \in (\mathcal{B}_2 + \gamma bB) \cap \mathcal{Z}_2$, the following holds*

$$|\phi(t, j)|_{\mathcal{B}_2} \leq c\,|\phi(0, 0)|_{\mathcal{B}_2} \exp(-\lambda t) \tag{18}$$

for all $(t, j) \in \operatorname{dom}\phi$.

Proposition 6. *Let Assumptions 1 and 2 hold and let K be given by* (10)*. For each compact set $\Omega \subset \mathbb{R}^6 \times \mathsf{SO}(3)$ there exist $k_i \in \mathbb{R}^2$ for all $i \in \{1, 2, 3\}$ and $c, \lambda > 0$ such that, for each solution ϕ to $\mathcal{H}_2$ with initial condition $\phi(0, 0) \in \mathcal{R}_2 \times \Omega \times \mathcal{Q}_2$, the* (18) *holds for all $(t, j) \in \operatorname{dom}\phi$.*

VI. Simulation Results

In this section, we present simulation results for the closed-loop systems that result from the interconnection between the dynamical system (3) and the controllers that are presented in Sections (V-A) and V-B. In these simulations, we consider that the acceleration of gravity is $g := (0, 0, 9.81)$ m/s^2 and that the thrust vector is given by $r := (0, 0, -1)$ in body-fixed coordinates. For controller design purposes, let us consider that the maximum acceleration and jerk are $(2\pi f)^2 r_\circ$ and $(2\pi f)^3 r_\circ$, respectively, corresponding to the acceleration and jerk of a circular trajectory of radius $r_\circ > 0$ and rotations per second $f \in \mathbb{R}$. Assumption 1 is satisfied with $\mathcal{R}_2 = \{\ddot{p_d} \in \mathbb{R}^3 : |\ddot{p_d}| \leq (2\pi f)^2 r_\circ\}$ and $\mathcal{R}_3 = \{\ddot{p_d} \in \mathbb{R}^3 : |\ddot{p_d}| \leq (2\pi f)^3 r_\circ\}$. Using the function σ in Example 1, we have that $|\sigma(u)| < |M|$ for each $u \in \mathbb{R}^3$, thus the bound

$$|T_i(\ddot{p_d}, e)| < m(|M| + |g| + (2\pi f)^2 r_\circ) \tag{19}$$

holds for the given reference trajectory and for all $i \in \{1, 2\}$, corresponding to the thrust commands (13) and V-B, respectively. Given that the quadrotor in our experimental setup weighs $m = 0.216$ kg and its thrust is limited to $T_{max} = 1.3m\,|g|$, it follows from (19) that M, $r_\circ$ and f must satisfy $|M| + (2\pi f)^2 r_\circ < 0.3\,|g|$ for the control signal to be within the actuator constraints. To strike a good balance between trajectory tracking and compensation of position/velocity tracking errors we restrict the analysis to reference trajectories whose acceleration does not exceed that of a circular path with a maximum acceleration equal to $0.1\,|g|$ and we select $M := 0.2\,|g|\,\mathbf{1}_3$ and $\ell := 0.1\,|g|\,\mathbf{1}_3$. Note that such choice implies that Assumption 2 is also satisfied.

We select the controller gain K as the solution to the LQR problem considering $R_{LQR} := I_3$ and $Q_{LQR} := \operatorname{diag}(\begin{bmatrix}\mathbf{1}_3^\top & 0.01\ \mathbf{1}_3^\top\end{bmatrix}^\top)$. More specifically, $K := -R_{LQR}^{-1} B^\top P_{LQR}$, where $P_{LQR} \succ 0_{6\times 6}$ is the solution to the Algebraic Riccati Equation

$$A^\top P_{LQR} + P_{LQR} A - P_{LQR} B R_{LQR}^{-1} B^\top P_{LQR} + Q_{LQR} = 0.$$

In order to test the controllers of Sections V-A and V-B, we carry out an input driven throw-and-catch maneuver for both closed-loop systems by means of a simulation that takes into consideration the dynamics of ω, given by $\dot{\omega} = 12\pi(\omega_i(p_d^{(3)}, z_i) - \omega)$ for each $i \in \{1, 2\}$. More specifically, we consider that the position reference is the origin of the inertial reference frame and that there is an open-loop command $\omega_d(t) = (18.5, 0, 0)$ rad/s for each $t \in [1, 1 + \pi/18.5]$ corresponding to a half flip around the body-fixed x-axis during which the trajectory tracking controller is switched off. The controllers are switched back on at $t \geq 1 + \pi/18.5$ s and we analyze the capabilities of each closed-loop system to stabilize the desired setpoint. The initial condition is $p(0, 0) = 0_3$, $v(0, 0) = 0_3$, $R(0, 0) = I_3$, the attitude control gains are $\alpha = 100$ and $\beta_1 = \beta_2 = 1$, and the function V_2 is given in Example 2. The initial values of the logic variables q_1 and q_2 are 1 and $-r$, respectively.

Figure 2 represents the attitude tracking error and the angular velocity from $t = 0.8$ s up to $t = 2$ s. The open-loop command $\omega_d(t)$ starts at $t = 1$ s and ends roughly at $t = 1.3$ s, as represented by the shaded region. It is possible to verify that: 1) the behavior of the closed-loop systems is indistinguishable up until the end of the half flip; 2) at the end of the half flip, the controller from Section V-A performs position stabilization in inverted flight while the controller from Section V-B has to perform another half flip to return to upright flight condition. Figure 3 represents the thrust commands for both controllers and it is possible to check that both signals are identical before the throw maneuver, but converge to symmetric values after the half flip. Note that immediately after the half flip, there is a time period in which the controller with no thrust reversal accelerates towards the ground leading to increased position tracking errors as represented in Figure 4.

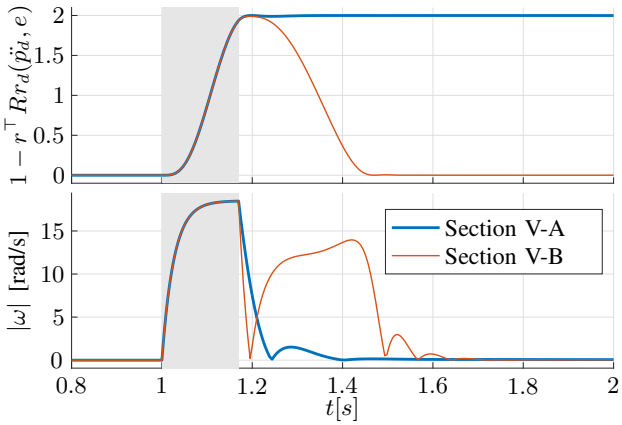

Fig. 2. Simulation results depicting the evolution over time of the distance of the thrust vector to the reference and of the angular velocity of the vehicle for a half flip. The shaded region spans the time in which open-loop command $\omega_d(t)$ is active.

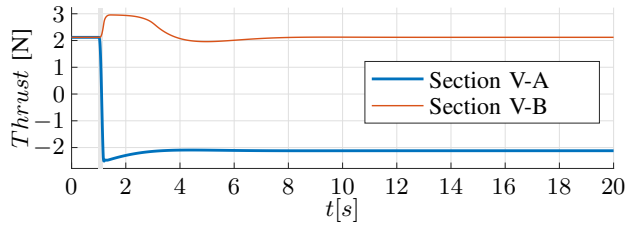

Fig. 3. Simulation results depicting the evolution over time of the commanded thrust. The shaded region spans the time in which open-loop command $\omega_d(t)$ is active.

VII. Conclusions

In this paper, we provided trajectory tracking controllers for multirotor aerial vehicles that are capable of operating with or without thrust reversal. We have shown that is possible to attain global asymptotic stabilization as well as semiglobal exponential stabilization of the zero error set in both operating modes. We compared the behaviour of the closed-loop systems by means of the simulation of a throw-and-catch maneuver, namely their ability to recover hovering flight from the disadvantaged conditions at the end of the maneuver. Further research on this topic will focus on the validation of the proposed controllers by means of experimental results.

References

[1] P. Ögren, E. Fiorelli, and N. Leonard, "Cooperative Control of Mobile Sensor Networks: Adaptive Gradient Climbing in a Distributed Environment," *IEEE Transactions on Automatic Control*, vol. 49, no. 8, pp. 1292–1302, 2004.

[2] M. Quaritsch, K. Kruggl, D. Wischounig-Strucl, S. Bhattacharya, M. Shah, and B. Rinner, "Networked UAVs as aerial sensor network for disaster management applications," *Elektrotechnik & Informationstechnik*, vol. 127, no. 3, pp. 56–63, 2010.

[3] B. J. Guerreiro, C. Silvestre, R. Cunha, and D. Cabecinhas, "LiDAR-Based Control of Autonomous Rotorcraft for the Inspection of Pier-like Structures," *IEEE Transactions on Control Systems Technology*, vol. 26, no. 4, pp. 1430–1438, 2018.

[4] P. M. Kornatowski, A. Bhaskaran, G. M. Heitz, S. Mintchev, and D. Floreano, "Last-Centimeter Personal Drone Delivery: Field Deployment and User Interaction," *IEEE Robotics and Automation Letters*, vol. 3, no. 4, pp. 3813–3820, 2018.

[5] L. R. G. Carrillo, A. E. D. López, R. Lozano, and C. Pégard, *Quad Rotorcraft Control: Vision-Based Hovering and Navigation*. Advances in Industrial Control, Springer London, 2012.

[6] A. L'Afflitto, R. B. Anderson, and K. Mohammadi, "An Introduction to Nonlinear Robust Control for Unmanned Quadrotor Aircraft: How to Design Control Algorithms for Quadrotors Using Sliding Mode Control and Adaptive Control Techniques [Focus on Education]," *IEEE Control Systems Magazine*, vol. 38, pp. 102–121, jun 2018.

[7] P. Pounds, R. Mahony, and P. Corke, "Modelling and control of a large quadrotor robot," *Control Engineering Practice*, vol. 18, no. 7, pp. 691–699, 2010.

[8] G. M. Hoffmann, H. Huang, S. L. Waslander, and C. J. Tomlin, "Precision flight control for a multi-vehicle quadrotor helicopter testbed," *Control Engineering Practice*, vol. 19, no. 9, pp. 1023–1036, 2011.

[9] K. Alexis, G. Nikolakopoulos, and A. Tzes, "Switching model predictive attitude control for a quadrotor helicopter subject to atmospheric disturbances," *Control Engineering Practice*, vol. 19, no. 10, pp. 1195–1207, 2011.

[10] T. Hamel, R. Mahony, R. Lozano, and J. Ostrowski, "Dynamic Modelling and Configuration Stabilization for an X4-Flyer.," *IFAC Proceedings Volumes*, vol. 35, no. 1, pp. 217–222, 2002.

[11] T. Lee, M. Leok, and N. H. McClamroch, "Nonlinear Robust Tracking Control of a Quadrotor UAV on SE(3)," *Asian Journal of Control*, vol. 15, no. 2, pp. 391–408, 2013.

[12] D. Mellinger, N. Michael, and V. Kumar, "Trajectory generation and control for precise aggressive maneuvers with quadrotors," *Springer Tracts in Advanced Robotics*, vol. 79, pp. 361–373, 2014.

[13] M.-D. Hua, T. Hamel, P. Morin, and C. Samson, "Control of VTOL vehicles with thrust-tilting augmentation," *Automatica*, vol. 52, pp. 1–7, 2015.

[14] R. Naldi, M. Furci, R. G. Sanfelice, and L. Marconi, "Robust Global Trajectory Tracking for Underactuated VTOL Aerial Vehicles Using Inner-Outer Loop Control Paradigms," *IEEE Transactions on Automatic Control*, vol. 62, no. 1, pp. 97–112, 2017.

[15] A. Tayebi and S. McGilvray, "Attitude stabilization of a VTOL quadrotor aircraft," *IEEE Transactions on Control Systems Technology*, vol. 14, no. 3, pp. 562–571, 2006.

[16] Y. Chen and N. O. Perez-Arancibia, "Lyapunov-based controller synthesis and stability analysis for the execution of high-speed multi-flip quadrotor maneuvers," *Proceedings of the American Control Conference*, pp. 3599–3606, 2017.

[17] M. D. Hua, T. Hamel, P. Morin, and C. Samson, "Introduction to feedback control of underactuated VTOL vehicles," *IEEE Control Systems*, vol. 33, no. 1, pp. 61–75, 2013.

[18] P. Casau, C. G. Mayhew, R. G. Sanfelice, and C. Silvestre, "Global exponential stabilization on the n-dimensional sphere," in *Proceedings of the 2015 American Control Conference (ACC)*, pp. 3218–3223, 2015.

[19] P. Casau, R. Sanfelice, R. Cunha, D. Cabecinhas, and C. Silvestre, "Robust global trajectory tracking for a class of underactuated vehicles," *Automatica*, vol. 58, pp. 90–98, 2015.

[20] P. Casau, C. G. Mayhew, R. G. Sanfelice, and C. Silvestre, "Robust global exponential stabilization on the n-dimensional sphere with applications to trajectory tracking for quadrotors," *Automatica*, vol. 110, 2019.

[21] R. Goebel, R. Sanfelice, and A. Teel, *Hybrid Dynamical Systems: Modeling, Stability, and Robustness*. Princeton University Press, 2012.

[22] P. Casau, R. Cunha, R. G. Sanfelice, and C. Silvestre, "Hybrid Control for Robust and Global Tracking on a Smooth Manifold," *IEEE Transactions on Automatic Control*, vol. PP, no. c, pp. 1–1, 2019.

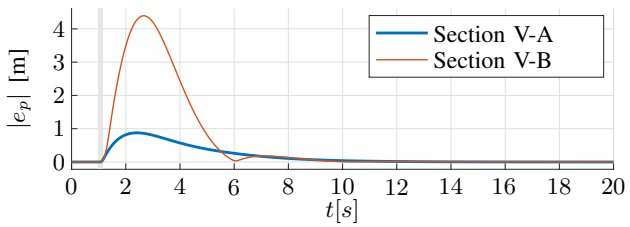

Fig. 4. Simulation results depicting the evolution over time of the position tracking error for a half flip. The shaded region spans the time in which open-loop command $\omega_d(t)$ is active.